X-ray Crystal Structure of a Xanthine Oxidase Complex with the Flavonoid Inhibitor Quercetin

ARTICLE *in* JOURNAL OF NATURAL PRODUCTS · JULY 2014

Impact Factor: 3.8 · DOI: 10.1021/np500320g

3 AUTHORS, INCLUDING:

Hongnan Cao
University of California, Riverside
9 PUBLICATIONS **73** CITATIONS
SEE PROFILE

James M Pauff
Vanderbilt University
11 PUBLICATIONS **225** CITATIONS
SEE PROFILE

JOURNAL OF NATURAL PRODUCTS

Article

pubs.acs.org/jnp

X-ray Crystal Structure of a Xanthine Oxidase Complex with the Flavonoid Inhibitor Quercetin

Hongnan Cao,[†] James M. Pauff,[‡] and Russ Hille*[,†]

[†]Department of Biochemistry, University of California, Riverside, California 92521, United States

[‡]Division of Hematology & Oncology, Vanderbilt University, Nashville, Tennessee 37232, United States

ABSTRACT: Xanthine oxidase catalyzes the sequential hydroxylation of hypoxanthine to uric acid via xanthine as intermediate. Deposition of crystals of the catalytic product uric acid or its monosodium salt in human joints with accompanying joint inflammation is the major cause of gout. Natural flavonoids are attractive leads for rational design of preventive and therapeutic xanthine oxidase inhibitors due to their beneficial antioxidant, anti-inflammatory, and antiproliferative activities in addition to their micromolar inhibitory activities toward xanthine oxidase. We determined the first complex X-ray structure of mammalian xanthine oxidase with the natural flavonoid inhibitor quercetin at 2.0 Å resolution. The inhibitor adopts a single orientation with its benzopyran moiety sandwiched between Phe 914 and Phe 1009 and ring B pointing toward the solvent channel leading to the molybdenum active center. The favorable steric complementarity of the conjugated three-ring structure of quercetin with the active site and specific hydrogen-bonding interactions of exocyclic hydroxy groups with catalytically relevant residues Arg 880 and Glu 802 correlate well with a previously reported structure−activity relationship of flavonoid inhibitors of xanthine oxidase. The current complex provides a structural basis for the rational design of flavonoid-type inhibitors against xanthine oxidase useful for the treatment of hyperuricemia, gout, and inflammatory disease states.

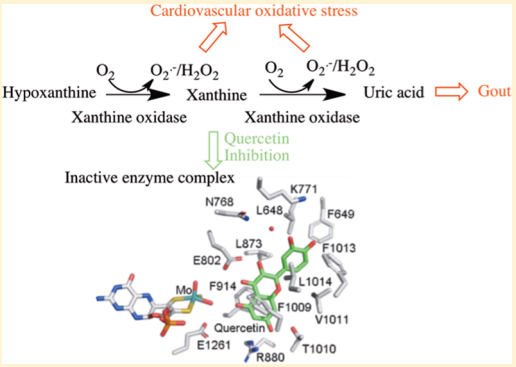

Xanthine oxidase is a molybdenum-containing enzyme that catalyzes the hydroxylation of sp^2-hybridized carbon centers of a wide variety of aromatic heterocycles, including the physiological purine substrates, hypoxanthine and xanthine, and aldehydes.[1−4] The vertebrate enzyme is a homodimer with each subunit containing four redox-active sites: an active-site molybdenum center, a pair of spinach ferredoxin-like [2Fe-2S] clusters, and FAD.[3,5] The overall catalytic sequence consists of a reductive half-reaction in which the substrate is oxidatively hydroxylated at the molybdenum center, reducing it from Mo(VI) to Mo(IV), and, after intramolecular electron transfer involving the intervening Fe/S centers, an oxidative half-reaction in which the reducing equivalents are removed from the enzyme via its FAD, with O_2 and NAD^+ serving as electron acceptors for the oxidase and dehydrogenase forms of the enzyme, respectively.[1,4]

Xanthine oxidase is not only necessary for normal human purine metabolism but is also implicated in multiple human diseases due to its ability to generate uric acid and reactive oxygen species. Deposition of crystals of uric acid or its monosodium salt in human joints with accompanying joint inflammation is the major cause of gout.[6] Xanthine oxidase is also thought to be involved in ischemia-reperfusion injury due to the elevated activity and production of superoxide and hydrogen peroxide by this enzyme.[7] In addition, xanthine oxidase has also been implicated in the development of various cardiovascular and inflammatory diseases. These implications stem from endothelial dysfunction and oxidative tissue injury due to an important fact that the enzyme is not only intracellular but also circulating in the blood. It has been shown to bind to vascular endothelium followed by endocytosis at remote tissues away from the origin of expression and release.[8−10] In particular, Landmesser and coauthors[11] reported a close association between increased activity of endothelium-bound xanthine oxidase and increased vascular oxidative stress in patients with chronic heart failure. Xanthine oxidase has been suggested to play a role in the pathogenesis of chronic heart failure via production of reactive oxygen species and regulating downstream pathways jointly with nitric oxide signaling.[12] Several studies have also pointed to the critical role of xanthine oxidase in the development of cardiomyopathy in type 1 diabetes by showing a preventative effect of allopurinol, a specific xanthine oxidase inhibitor. Desco and coauthors[13] demonstrated that treatment with allopurinol effectively decreased oxidative stress in plasma of type 1 diabetic patients and experimental diabetes. Rajesh and coauthors[14] reported that allopurinol improved systolic and diastolic performance of heart function in streptozotocin-induced diabetic mice accompanied by attenuation of diabetes-induced increase of myocardial, liver, and serum xanthine oxidase activity, myocardial reactive oxygen species, nitrotyrosine generation, inducible nitric oxide synthase expression, apoptosis, poly-

Received: April 10, 2014
Published: July 1, 2014

(ADP-ribose) polymerase activity, and fibrosis. Thus, the regulated activity of xanthine oxidase in the human body is important for human health and the prevention of disease. Various inhibitors of xanthine oxidase have been developed in the past 50 years, the progress of which has been extensively reviewed.[15,16]

Two inhibitors of xanthine oxidase, allopurinol and febuxostat, have been approved by the Food and Drug Administration to treat gout (Figure 1). Allopurinol, a

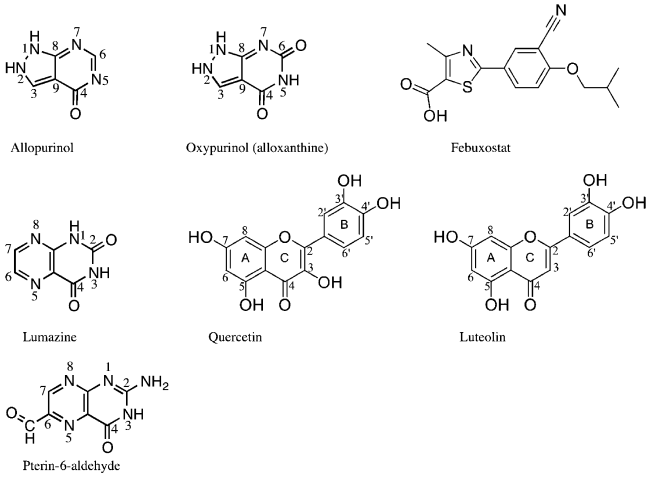

Figure 1. Chemical structures of various inhibitors of xanthine oxidase and substrate lumazine. Allopurinol and febuxostat are FDA-approved drugs for the treatment of gout. Oxypurinol (alloxanthine) is the hydroxylation product of allopurinol by xanthine oxidase and inhibits xanthine oxidase via direct coordination of its N2 atom to Mo of the enzyme active site. Quercetin and luteolin are natural flavonoids commonly found in plants and inhibitors of xanthine oxidase. Lumazine is structurally analogous to the benzopyran moiety of quecetin and luteolin (rings A and C). Pterin-6-aldehyde is a competitive inhibitor of xanthine oxidase. The various ring-numbering schemes for the heterocycles are also indicated.

mechanism-based inhibitor of xanthine oxidase, was developed in 1963 by Gertrude B. Elion and George H. Hitchings, who were awarded the 1988 Nobel Prize in Physiology or Medicine for their work. Allopurinol itself competitively inhibits xanthine oxidase with a reported K_i of 100−700 nM for human and several other vertebrate enzymes.[17] However, its hydroxylation product by xanthine oxidase, oxypurinol, also known as alloxanthine, strongly inhibits the reduced form of the enzyme with an overall K_i of 35 nM and weakly inhibits oxidized xanthine oxidase with a reported K_i of ∼1 μM (Figure 2).[17,18] Febuxostat was approved by the FDA in 2009 and is a structure-based mixed-type inhibitor with K_i and K_i' values of 120 pM and 900 pM, respectively, for bovine xanthine oxidase,[14] which conserves all the catalytically essential residues of the human enzyme with 90% overall sequence identity. Febuxostat sterically complements the solvent-accessible substrate channel leading to the enzyme active site and forms multiple interactions with the channel (Figure 2).[19]

Quercetin is a natural flavonol commonly found in plants, including vegetables, fruits, and tea (Figure 1). It has been shown to have antioxidant, anti-inflammatory, and antiproliferative activities not only due to its ability to scavenge reactive oxygen species but also by direct modulation of gene expression.[20] For example, several in vitro studies using different cell lines have shown that quercetin inhibits LPS-

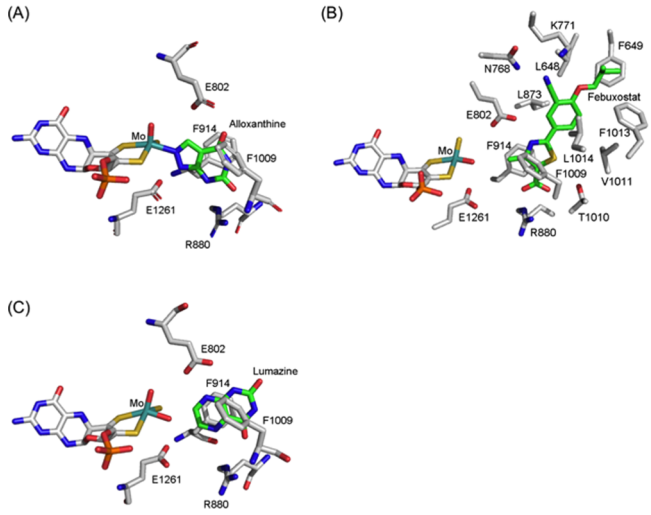

Figure 2. Reported crystal structures of bovine xanthine oxidoreductase in complex with alloxanthine,[43] febuxostat,[19] and lumazine.[39] (A) Alloxanthine forms a direct Mo−N bond with the molybdenum center of the enzyme in addition to having multiple hydrogen-bonding and van der Waals interactions with active site residues (PDB code: 3BDJ).[43] (B) Febuxostat forms multiple noncovalent interactions with the active site amino residues and almost completely fills the substrate-entering channel leading to the molybdenum center (PDB code: 1N5X).[19] (C) Lumazine binds at the molybdenum active site with C4═O hydrogen bonded to Arg 880 (PDB code 3ETR).[39] Carbon is in white for the enzyme and green for the inhibitors or the substrate, nitrogen in blue, oxygen in red, sulfur in yellow, phosphorus in gold, and molybdenum in teal. Residue numbers are also shown.

induced cytokine production (TNF-α in macrophages and IL-8 in lung cells).[20] Another recent study has implicated quercetin as sensitizing ovarian cancer cells to death by TNF-related apoptosis-inducing ligand (TRAIL).[21] Quercetin has also been reported to inhibit cell proliferation by interacting with estrogen-binding sites.[20] The structures of many proteins in complex with quercetin have been reported in the Protein Data Bank (PDB) at www.rcsb.org (Table 1), several of which are associated with its in vitro or vivo activities.[22−38] Interestingly, several in vitro kinetic studies have shown that quercetin is a significant inhibitor of xanthine oxidase. Nagao and coauthors[22] have demonstrated that quercetin is a mixed-type inhibitor with a K_i of 0.28 μM at 37 °C and pH 7.8. They have proposed that quercetin and other structurally analogous flavonoids inhibit xanthine oxidase by interacting with the enzyme at a site other than the molybdenum center. On the other hand, the results from Pauff and coauthors[23] have suggested that quercetin competitively inhibits xanthine oxidase activity to hydroxylate xanthine as well as generate superoxide with a K_i of 1.2 μM at 25 °C and pH 7.4. On the basis of the structural similarity between the benzopyran moiety of quercetin and lumazine,[39] whose orientation in the active site has been determined crystallographically (Figure 2), it has been proposed that quercetin and the related natural compound luteolin bind at the active site molybdenum center, with their benzopyran rings intercalated between conserved phenylalanine residues Phe 914 and Phe 1009 and their exocyclic carbonyl groups directed toward Arg 880.[23] In the present work, we have determined the crystal structure of xanthine oxidase in complex with quercetin at 2.0 Å resolution and established the binding mode of quercetin with its benzopyran moiety sandwiched between Phe 914 and Phe 1009, ring A directed toward the molybdenum

dx.doi.org/10.1021/np500320g | J. Nat. Prod. 2014, 77, 1693−1699

Table 1. Reported Structures of Protein−Quercetin Complexes[a]

PDB ID	protein (organism)	protein family/function	quercetin activity
4LMU[24]	Pim1 (human)	Ser/Thr-protein kinase (proto-oncogene)	competitive inhibitor
4DFU[25]	APH(2″)-Iva (*Enterococcus casseliflavus*)	aminoglycoside kinase (antibiotic resistance)	competitive inhibitor
3NVY	xanthine oxidase (bovine)	purine oxidation (uric acid and ROS producer)	competitive/mixed type inhibitor[16,17]
3LJ0[26]	IRE1 (*S. cerevisiae*/yeast)	Ser/Thr-protein kinase/endoribonuclease	coactivator of RNase
3LM5[27]	STK17B (human)	Ser/Thr-protein kinase (phosphorylate myosin)	N.A.[b]
3CF8[28]	FabZ (*Helicobacter pylori*)	β-hydroxyacyl−acyl carrier protein dehydratase	competitive inhibitor
3BXX[29]	DFR (*Vitis vinifera*/grape)	dihydroflavonol 4-reductase	competitive inhibitor
3BPT[30]	3-hydroxyisobutyryl-CoA hydrolase (human)	β-hydroxyisobutyryl-CoA hydrolase	N.A.[b]
2JJ2[31]	F1-ATPase (bovine)	mitochondrial F_1F_o-ATPase	inhibitor of ATP hydrolysis not synthesis
2UXH[32]	TTGR (*Pseudomonas putida*)	multidrug binding/HTH-type transcription regulator	binding and increase antimicrobial tolerance
2O3P[33]	Pim1 (human)	Ser/Thr-protein kinase (proto-oncogene)	competitive inhibitor
2C9Z[34]	VvGT1 (*Vitis vinifera*)	UDP-glucose:flavonoid glycosyltransferase dehydratase	substrate (glycosyl acceptor)
1H1I[35]	2,3QD (*Aspergillus japonicus*)	quercetin 2,3-dioxygenase (copper-dependent)	substrate (two CC bonds breakage of heterocycle)
1GP6[36]	ANS (*Arabidopsis thaliana*)	anthocyanidin synthase (2-oxoglutarate iron-dependent dioxygenase)	product from oxidation of dihydroquercetin
1E8W[37]	PI3K (*Sus scrofa*/wild boar)	phosphoinositide 3-kinase (PIP3/signal producer)	competitive inhibitor
2HCK[38]	HCK (human)	Src-family tyrosine kinase (proto-oncogene)	potent inhibitor

[a]Protein Data Bank http://www.rcsb.org. [b]Information not available.

cofactor, and ring C projecting into the solvent channel in agreement with the orientation previously proposed by Pauff and coauthors.[23] On the other hand (Figure 2), we find that the C-4 carbonyl and C-5 hydroxy groups of quercetin are within hydrogen-bonding distance of the side chain carboxy group of Glu 802 rather than Arg 880 and that the C-7 hydroxyl group is, instead, within hydrogen-bonding distance of the guanidinium group of Arg 880. This structural study corroborates the results of previous kinetic studies that have suggested quercetin is a biologically active molecule that targets xanthine oxidase, and provides a plausible structural basis of inhibition of the enzyme. We discuss the rational design of inhibitors of xanthine oxidase in the context of the observed orientation of the flavonoid inhibitor quercetin. We also extend our conclusions to suggest future structural and mechanistic studies of other natural compounds, given the prevalence of cell-based and in vitro evidence of these compounds as beneficial to human health and disease.

RESULTS AND DISCUSSION

Overall Crystal Structures of Xanthine Oxidase in Complex with Quercetin. The overall protein structure of quercetin-complexed xanthine oxidase at 2.0 Å resolution is found to be similar to that reported for the oxidized enzyme,[5,39−42] with differences limited to the active site. Table 2 summarizes the structural refinement statistics. Figure 3 shows the two active sites of the asymmetric unit overlaid with the F_o-F_c omit map contoured at 3σ and the $2F_o-F_c$ omit map at 1σ (the map omitted quercetin).

Orientation of Quercetin in the Molybdenum Active Site of Xanthine Oxidase. Strong positive electron density in the F_o-F_c omit map in both active sites of the crystallographic asymmetric unit supports a single orientation of quercetin with its benzopyran moiety adjacent to the molybdenum center and its 3,4-dihydroxyphenyl moiety pointing toward the solvent access channel. No electron density is observed connecting the Mo−OH and quercetin, suggesting that no catalysis has occurred. A closer examination of the binding mode of quercetin in the active site reveals multiple favorable interactions of the inhibitor with active site residues and the molybdenum center. There are two major types of interactions: first, van der Waals interactions between the conjugated ring structures of quercetin and the active site phenylalanine residues; and second, hydrogen-bonding or polar interactions between exocyclic oxo or hydroxy groups of quercetin and the active site polar residues. These are discussed further below.

Table 2. Statistics for Data Collection and Structural Refinement[a]

statistic	XO with quercetin
Protein Data Bank code	3NVY
space group	$P2_1$
cell dimensions	
a, *b*, *c* (Å)	132.7, 73.4, 138.2
α, *β*, *γ* (deg)	90.0, 97.1, 90.0
resolution (Å)	101.5−2.0
wavelength (Å)	0.9793
unique reflns (test set)	175 239 (8835)
completeness % (highest resolution shell, Å)	98.2 (98.6)
I/σ (highest resolution shell)	17.5 (1.9)
R_{cryst} (highest resolution shell)	19.2 (21.5)
R_{free} (highest resolution shell)	23.7 (26.6)
Ramachandran statistics (%)	89.6, 9.7, 0.4, 0.2
mean coordinate error based on free *R* value (Å)	0.170
mean coordinate error based on maximum likelihood (Å)	0.123
rmsd bond length (Å)	0.015
rmsd bond angles (deg)	1.6
average *B* value (Å^2)	26.7
number of non-hydrogen atoms in refinement	20 401
number of waters	1057

[a]Ramachandran statistics indicate the percentage of residues in the most favored, additionally allowed, generously allowed, and disallowed regions of the Ramachandran diagram as defined by the program PROCHECK.[57] I/σ is defined as the ratio of averaged value of the intensity to its standard deviation.

Active Site Hydrophobic Residues Determine the Overall Binding Mode of Quercetin. Rings A, B, and C of quercetin are defined in Figure 1. In the current crystal structure, rings A and C are coplanar and sandwiched between

dx.doi.org/10.1021/np500320g | J. Nat. Prod. 2014, 77, 1693−1699

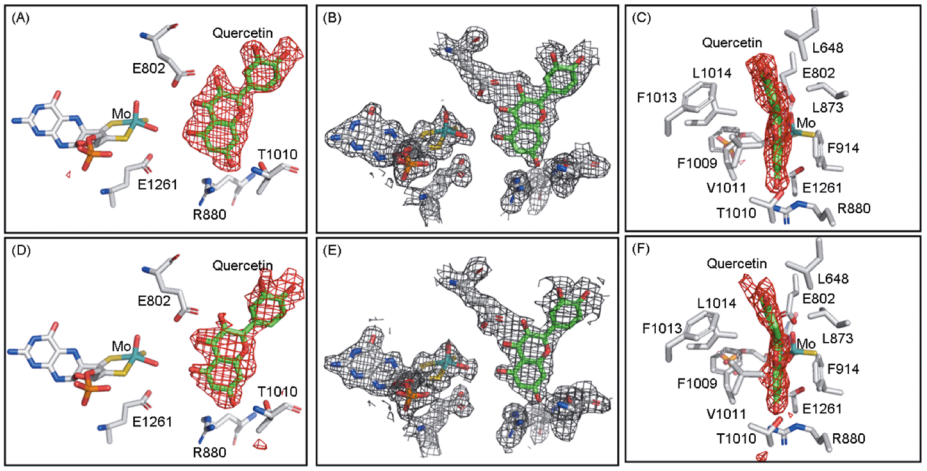

Figure 3. Active sites of xanthine oxidase complexed with quercetin. (A), (B), and (C) show one active site of the asymmetric unit, while (D), (E), and (F) show the other. (A), (C), (D), and (F) have F_o-F_c omit maps contoured at 3.0 σ, and (B) and (E) have $2F_o-F_c$ omit maps contoured at 1.0 σ all within 2.0 Å of all atoms shown. (C) and (F) are rotated approximately 90° about the vertical axis from the perspective shown in (A) and (D), respectively. Some of the residues in (C) and (F) are not displayed in (A), (B), (D), and (E) for clarity. The maps were constructed without quercetin and overlaid with the final model. Carbon is in white for the enzyme and green for quercetin, nitrogen in blue, oxygen in red, sulfur in yellow, phosphorus in gold, and molybdenum in teal. Residue numbers are also shown.

conserved active site phenylalanine residues Phe 914 and Phe 1009 in a manner similar to the binding modes seen with all substrates/analogues of the enzyme (Figure 4A and B).

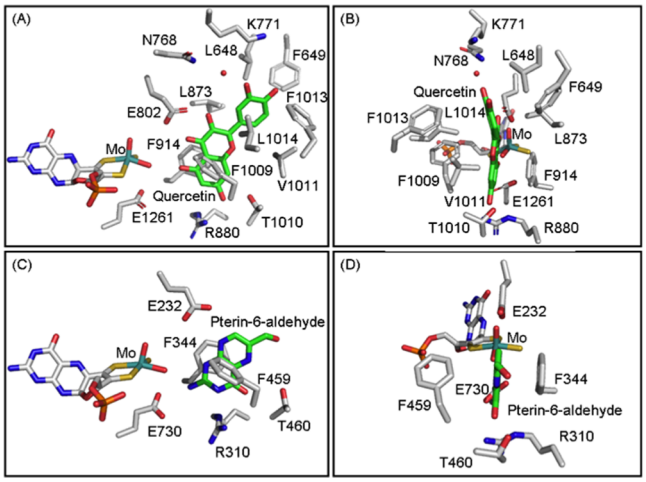

Figure 4. Comparison of molybdenum active sites of the structures of bovine xanthine oxidase in complex with quercetin (top) and *R. capsulatus* xanthine dehydrogenase in complex with pterin-6-aldehyde (bottom). The latter was reported by Dietzel and coauthors.[42] PDB codes are 3NVY and 2W54 for the two structures, respectively. (B) and (D) are rotated approximately 90° about the vertical axis from the perspective shown in (A) and (C), respectively. Carbon is in white for the enzyme and green for quercetin and pterin-6-aldehyde, nitrogen in blue, oxygen in red, sulfur in yellow, phosphorus in gold, and molybdenum in teal. Residue labels are also shown.

Additional potential van der Waals interactions are also observed between ring C and hydrophobic residues Leu 873, Leu 1014, Leu 648, Val 1011, and Phe 1013. The binding mode of the fused rings A and C of quercetin that are sandwiched between Phe 914 and Phe 1009 resembles that of pterin-6-aldehyde (between Phe 344 and Phe 459 of *R. capsulatus* xanthine dehydrogenase, Figure 4).[42] However, the orientation of quercetin is different from that of alloxanthine[38] (Figure 2A) and lumazine[41] (Figure 2C) in that rings A and C of quercetin are rotated between Phe 914 and Phe 1009 almost 90° relative to the orientation of the two rings of lumazine at the active site of xanthine oxidase.

Specific Conformation of Quercetin at the Molybdenum Active Site of Xanthine Oxidase. In the structure of the quercetion complex, the clear electron density associated with bound inhibitor clearly suggests a dihedral angle of around 154.5° between rings B and C (155.6° and 153.3° for quercetin molecules at the two active sites, respectively), as shown in Figure 3C and F. Cornard and coauthors[44] have studied the conformation of quercetin both in the solid state and in vacuo using semiempirical calculations combined with vibrational and electronic spectroscopy. Their results suggest that in quercetin the lowest energy rotamers about the bond between rings B and C possess dihedral angles θ of 27° and 153° between the two rings (θ = 0° for quercetin in Figure 1). Thus, the observed conformation of bound quercetin (θ = 154.5°) in the current crystal structure is an energetically favorable conformation. It also appears that the twisting between rings B and C is directed by the shape of the active site as defined by the two phenylalanine residues as shown in Figure 4A and B.

Although there appears to be no direct interaction of the 3′- and 4′-hydroxy groups of quercetin with active site residues, the existence of polar residues Asn 768 and Lys 771 in proximity to the 3′-hydroxy group likely directs quercetin into the observed conformation (Figure 4A and B). The distance from the side chain amide nitrogen of Asn 768 to the 3′-OH of quercetin is 5.40 and 5.52 Å in the two active sites of the asymmetric unit, respectively, and the corresponding distances are 4.60 and 4.68 Å from the side chain amino nitrogen of Lys 771. All of these distances are too long to support hydrogen bonding, although in one active site of the current structure we observe a water molecule bridging Asn 768 and the 3′-OH of quercetin through hydrogen bonds. These results are generally consistent with kinetic studies indicating little difference in inhibition of xanthine oxidase activity between quercetin and kaempferol, the latter of which lacks a 3′-hydroxy group.[22,45] Both Asn 768 and Lys 771 in bovine xanthine oxidase are conserved in human

dx.doi.org/10.1021/np500320g | *J. Nat. Prod.* 2014, 77, 1693−1699

xanthine oxidase corresponding to Asn 769 and Lys 772, respectively.

Hydrogen-Bonding Interactions of Quercetin with the Active Site of Xanthine Oxidase. The 7-OH group of quercetin is within hydrogen-bonding distance of not only two nitrogen atoms (ε and η) of the side chain guanidinium group of Arg 880 (3.23 and 2.73 Å for one active site and 3.22 and 2.77 Å for the other) but also the side chain hydroxy group of Thr 1010 (2.87 and 2.66 Å for the two active sites, respectively). Previous structure−activity studies of flavonoids as inhibitors of xanthine oxidase by Nagao and coauthors[22] have shown that methylation of the 7-OH group of quercetin leads to at least a 100-fold increase in IC_{50}, in agreement with our observation of multiple favorable interactions of the 7-OH group with active site residues of the enzyme. In addition, the C-4 carbonyl group is within hydrogen-bonding distance of both oxygens of Glu 802, i.e., 2.61 and 2.65 Å for one active site and 2.36 and 2.73 Å for the other. The 5-OH group points toward and is within hydrogen-bonding distance of the equatorial Mo-OH group, i.e., 3.16 and 3.00 Å in the two active sites, respectively. However, Cos and coauthors[45] have shown that loss of the C-5 hydroxyl group of quercetin only moderately compromises the IC_{50} value, by less than a factor of 2. It is the hydrogen-bonding interactions with Arg 880, Thr 1010, Glu 802, and Mo-OH that appear to control the overall orientation of quercetin, in particular, the interactions of the 7-OH group with Arg 880 and Thr 1010.

Interestingly, the 3-OH group of quercetin has an extremely short distance to one of the oxygen atoms of the side chain carboxylic group of Glu 802, i.e., 2.05 and 2.07 Å for the two active sites, respectively. In addition, in the current structure at 2.0 Å resolution the electron density in the F_o-F_c omit map is not sufficiently unequivocal to identify the exact orientation of Glu 802 and the C-3 and C-4 exocyclic oxygens of quercetin (Figure 3B and E). Further, the B factors for the C-3 oxygen of quercetin and the nearest side chain oxygen from Glu 802, i.e., 37.53 and 36.26 $Å^2$ for one active site and 37.02 and 30.15 $Å^2$ for the other, are relatively large compared to the average B factor for the whole structure (26.7 $Å^2$). Thus, given the less well-defined electron density and relatively large B factors for these atoms, there is some ambiguity as to the hydrogen bond distance between the C-3 oxygen of quercetin and Glu 802. The 3-OH group of quercetin appears to contribute little to its inhibitory capacity. Still, Nagao and coauthors[22] have demonstrated that quercetin and luteolin, lacking the 3-OH group, are both mixed-type inhibitors of xanthine oxidase with similar K_i values of 0.28 and 0.31 μM, respectively, at 37 °C and pH 7.8. On the other hand, the results of Pauff and coauthors[23] suggest that quercetin and luteolin are competitive inhibitors of xanthine oxidase, with K_i values of 1.2 and 1.9 μM, respectively, at 25 °C and pH 7.4. These studies suggest that even if there was a hydrogen bond between the 3-OH group of quercetin and the side chain of Glu 802, the interaction is relatively weak.

Rational Design of Flavonoid-Type Xanthine Oxidase Inhibitors. On the basis of the present crystal structure of the xanthine oxidase−quercetin complex, it is evident that favorable van der Waals interactions between the three rings of inhibitor and hydrophobic residues of the enzyme active site contribute to overall inhibitor binding and thus the binding specificity of this inhibitor (Figure 4). It is likely that the aromaticity of rings A and B as well as conjugation between these rings both contribute to the overall steric match between quercetin and the binding pocket and thus tight binding. This is consistent with the kinetic studies performed by Cos and coauthors[45] suggesting the importance of the 2,3-double-bond flavonoids in inhibiting xanthine oxidase activity. We also observe potentially favorable hydrogen-bonding interactions between the 7-OH group and both Arg 880 and Thr 1010, consistent with the previous kinetic studies of Nagao and coauthors.[22] The potential hydrogen-bonding interactions between the 5-OH group and the Mo-OH group likely help orient quercetin but appear not to contribute significantly to its tight binding, as reflected in the previous kinetic studies of Cos and coauthors.[45] The current crystal structure suggests that the C-4 carbonyl and 3-OH group of quercetin are involved in hydrogen-bonding interactions with the side chain carboxylic group of Glu 802, although multiple kinetic studies comparing the effectiveness of quercetin and luteolin suggest that the 3-OH group does not contribute significantly to binding affinity.[22,23,45]

For rational design of flavonoid-type inhibitors of xanthine oxidase, the following considerations constitute a good starting point: (i) the conjugated three-ring backbone of quercetin seems desirable and complements the shape of the active site and solvent channel; (ii) a 7-OH group is likely essential for effective inhibition, and its interaction with the conserved Arg 880 is similar to interactions previously observed for the C-6 carbonyl groups of the physiological substrate hypoxanthine and xanthine, which are thought to be essential for transition state stabilization during catalysis;[39−41,46] (iii) exocyclic carbonyl or hydroxy groups at C-3, C-4, and C-5 positions may be subject to modification to enhance inhibition. For example, replacement of the C-4 and C-5 hydroxy groups of quercetin with an amino group may increase binding affinity through stronger interactions with the side chain carboxylic group and Mo-OH. This suggestion is inspired by the observation of a single nonproductive orientation of guanine in the active site of xanthine oxidase, which precludes formation of the highly mutagenic 8-hydroxyguanine and is likely determined by favorable interactions between the C-2 amino group and both Glu 802 and Mo-OH.[47] In addition, pterin-6-aldehyde, a potent inhibitor of xanthine oxidase, i.e., a K_i value of 1.78 nM for bovine xanthine oxidase and 103.57 nM for *R. capsulatus* xanthine dehydrogenase, also binds with its C-2 amino group within hydrogen bonding distance of Mo-OH, as shown in Figure 4.[42] On the other hand, modification at C-5 with exocyclic functional groups that may form a covalent interaction with the molybdenum center such as is seen with alloxanthine, is another direction that might lead to more potent inhibitors of xanthine oxidase. (iv) Although the 3′- and 4′-hydroxy groups of quercetin may not contribute significantly to its inhibitory effect on xanthine oxidase, their presence is likely important for effective superoxide scavenging activity.[45] Consequently, the optimization of flavonoid inhibitors against xanthine oxidase may require taking into account both the potency of the inhibition of xanthine oxidase and their direct antioxidant activity, as well as the safety and pharmacological profiles in evaluating overall efficacy.

In summary, the current crystal structure of the xanthine oxidase−quercetin complex clearly demonstrates a single orientation of the inhibitor with its benzopyran moiety sandwiched between Phe 914 and Phe 1009 and ring B pointing toward the solvent channel. The tight binding of quercetin to xanthine oxidase is likely due to a combination of steric complementarity and favorable van der Waals interactions between the conjugated tricyclic structure of quercetin and specific active site residues. The key residues responsible

for querectin interaction revealed in the current structure are generally conserved both structurally and in sequence between bovine and human enzymes.[48] These include the catalytically important residues Arg 880/881 and Glu 802/803, as well as residues involved in purine substrate binding, i.e., Phe 914/915, Phe 1009/1010, and Thr 1010/1011, and also residues forming the extended solvent-accessible channel leading to the molybdenum center, i.e., Leu 873/874, Leu 1014/1015, Val 1011/1012, and Phe 1013/1014 (here residues are numbered for bovine/human enzymes). The overall binding mode and interactions of quercetin with xanthine oxidase are analogous to the FDA-approved drug febuxostat despite their structural difference. It is to be emphasized that additional interactions may be explored to enhance the specificity and potency of xanthine oxidase inhibitors by extending the binding pocket to species-specific residues Leu 648/Ile 649 and Phe 649/Cys 650 (bovine/human) near the gate of the channel and distal from the active site where there may be less evolutionary pressure. The current complex provides a structural basis for the rational design and optimization of flavonoid-type inhibitors against xanthine oxidase that could be used in the treatment of hyperuricemia, gout, and inflammatory disease states. This work illustrates the utility of combining structural data with kinetic analysis to provide a rational basis for the development of additional therapeutics modeled after natural products.

EXPERIMENTAL SECTION

Materials. Magnetic bases for use with the automated crystallography system at the LRL-CAT of Argonne National Laboratory were obtained from MAR-USA (Evanston, IL, USA). Mounted cryoloops, magnetic cryovials, and crystal growth materials were obtained from Hampton Research (Aliso Viejo, CA, USA). Polyethylene glycol 200 (PEG 200) and PEG 8000 stock solutions were obtained from Hampton Research. All other chemicals and reagents were obtained at the highest quality/purity available from Sigma-Aldrich or Fisher Scientific and used without further purification.

Purification of Bovine Xanthine Oxidoreductase. Bovine xanthine oxidoreductase was purified from fresh, unpasteurized bovine milk (Scott Brothers Dairy, Chino, CA, USA) as described elsewhere.[49] In order to eliminate possible problems due to genetic heterogeneity in the dairy herd, the enzyme used for crystallography was isolated from milk obtained from an individual cow. The purified enzyme exhibited a ratio of absorbance at 280 and 450 nm of 6.0−6.8 and a percentage of functionality of 30−60% due to variability in the amount of the nonfunctional desulfo form of the enzyme present in which a catalytically essential Mo=S group has been replaced by a second Mo=O group in the molybdenum coordination sphere. The percentage of functionality was determined as described by Massey and Edmondson.[50] A folate affinity column procedure[51] was used as a final purification step to enrich the functionality to above 80%. Purified enzyme was made 1.0 mM in sodium salicylate, stored in liquid nitrogen, and passed down a Sephadex G-25 column to remove salicylate prior to use.

Crystallization, Data Acquisition, and Structure Determination. Xanthine oxidoreductase crystals were grown using the batch method according to published methods using microbridges to hold batch solutions in sealed wells of a 24-well tray.[38−41] Batch solutions contained 10 μL of a 34.5 μM (5 mg/mL) enzyme solution mixed with 5 or 6 μL of a 12% polyethylene glycol 8000 precipitant solution. Throughout this work, the enzyme concentration refers to total monomer concentration based on an extinction coefficient at 450 nm of 37.8 mM^{-1} cm^{-1}.[49]

Crystals were grown in the dark at 25 °C for 2−3 days before harvesting. A 42% solution of polyethylene glycol 200 was used as cryoprotectant. Quercetin was introduced to xanthine oxidoreductase crystals via soaking to reach a final concentration of quercetin of 5 mM in the crystal well. Excess quercetin (compared to 0.28−1.2 μM K_i previously reported[22,23]) was applied to accelerate diffusion of the ligand to the active site of xanthine oxidase and ensure its saturation in the crystal form of the enzyme. After soaking quercetin for 5−10 min, crystals were mounted and flash-frozen in liquid nitrogen. Diffraction data were collected at Argonne National Laboratory on the LRL-CAT beamline using a wavelength of 0.9793 Å and a MARCCD 165 detector. Data sets were collected to a resolution of 2.0 Å for both structures reported here.

Crystallographic data were processed using the MOSFLM package of the CCP4 program suite.[52] The structure of each complex was determined by molecular replacement using the MOLREP package of CCP4 with the previously reported crystal structure of xanthine oxidoreductase of Enroth and coauthors[5] as the search model (Protein Data Bank code 1FIQ). The output structure was refined first by rigid body refinement and subsequently by restrained refinement using the REFMAC program of the CCP4 suite.[52,53] The weighting term for geometric restraints was adjusted in REFMAC to minimize R_{cryst} while at the same time minimizing the difference between R_{cryst} and R_{free}. No noncrystallographic symmetry restraints were used during refinement of the structures. Water molecules were added to both the crystal structures (using REFMAC) prior to building in the substrates.

Structure files for quercetin were constructed using the PRODRG2 server,[54] and the respective Protein Data Bank codes were built into the corresponding $2F_o-F_c$ and F_o-F_c omit electron density maps observed in the active sites using COOT.[55] After merging the substrate structure files with those for the respectively refined protein structures, the results were refined again using the restrained refinement mode in REFMAC. Similar to our published structures of xanthine oxidase, residues 1316−1326 were added to the terminus of one of the two monomers in the asymmetric unit to model clear extra electron density for them. The final structure files were deposited into the Protein Data Bank (PDB) at www.rcsb.org; the PDB accession number is 3NVY. All structures in the figures have been rendered using PyMol.[56]

AUTHOR INFORMATION

Corresponding Author

*E-mail: russ.hille@ucr.edu. Tel: 951-827-6354. Fax: 951-827-2364.

Notes

The authors declare no competing financial interest.

ACKNOWLEDGMENTS

This work was supported by a grant from the Basic Energy Sciences program of the Department of Energy (DE-FG02-13ER16411). We thank Dr. T. Nishino for advice in the use of the folate column procedure and for helpful discussions. Use of the Advanced Photon Source at Argonne National Laboratory was supported by the U.S. Department of Energy, Office of Science, Office of Basic Energy Sciences, under Contract No. DE-AC02-06CH11357. Use of the Lilly Research Laboratory Collaborative Access Team (LRL-CAT) beamline at Sector 31 of the Advanced Photon Source was provided by Eli Lilly & Company, who operates the facility.

REFERENCES

(1) Hille, R. *Chem. Rev.* **1996**, *96*, 2757−2816.
(2) Hille, R. *Trends Biochem. Sci.* **2002**, *27*, 360−367.
(3) Hille, R.; Nishino, T. *FASEB. J.* **1995**, *9*, 995−1003.
(4) Hille, R. *Arch. Biochem. Biophys.* **2005**, *433*, 107−116.
(5) Enroth, C.; Eger, B. T.; Okamoto, K.; Nishino, T.; Nishino, T.; Pai, E. F. *Proc. Natl. Acad. Sci. U.S.A.* **2000**, *97*, 10723−10728.
(6) Choi, H. K.; Mount, D. B.; Reginato, A. M. *Ann. Int. Med.* **2005**, *143*, 499−516.
(7) Meneshian, A.; Bulkley, G. B. *Microcirculation* **2002**, *9*, 161−175.
(8) Berry, C. E.; Hare, J. M. *J. Physiol.* **2004**, *555*, 589−606.
(9) Boueiz, A.; Damarla, M.; Hassoun, P. M. *Am. J. Physiol. Lung Cell Mol. Physiol.* **2008**, *294*, L830−L840.

(10) Houston, M.; Estevez, A.; Chumley, P.; Aslan, M.; Marklund, S.; Parks, D. A.; Freeman, B. A. *J. Biol. Chem.* **1999**, *274*, 4985−4994.
(11) Landmesser, U.; Spiekermann, S.; Dikalov, S.; Tatge, H.; Wilke, R.; Kohler, C.; Harrison, D. G.; Hornig, B.; Drexler, H. *Circulation* **2002**, *106*, 3073−3078.
(12) Ungvari, Z.; Gupte, S. A.; Rkai, S.; Recchia, F. A.; Batkai, S.; Pacher, P. *Curr. Vasc. Pharmacol.* **2005**, *3*, 221−229.
(13) Desco, M. C.; Asensi, M.; Marquez, R.; Martinez-Valls, J.; Vento, M.; Pallardo, F. V.; Sastre, J.; Vina, J. *Diabetes* **2002**, *51*, 1118−1124.
(14) Rajesh, M.; Mukhopadhyay, P.; Batkai, S.; Mukhopadhyay, B.; Patel, V.; Hasko, G.; Szabo, C.; Mabley, J. G.; Liaudet, L.; Pacher, P. *J. Cell. Mol. Med.* **2009**, *13*, 2330−2341.
(15) Borges, F.; Fernandes, E.; Roleira, F. *Curr. Med. Chem.* **2002**, *9*, 195−217.
(16) Pacher, P.; Nivorozhkin, A.; Szabo, A. C. *Pharmacol. Rev.* **2006**, *58*, 87−114.
(17) Elion, G. B. *Ann. Rheum. Dis.* **1966**, *25*, 608−614.
(18) Williams, J. W.; Bray, R. C. *Biochem. J.* **1981**, *195*, 753−760.
(19) Okamoto, K.; Eger, B. T.; Nishino, T.; Kondo, S.; Pai, E. F.; Nishino, T. *J. Biol. Chem.* **2003**, *278*, 1848−1855.
(20) Boots, A. W.; Haenen, G. R.; Bast, A. *Eur. J. Pharmacol.* **2008**, *585*, 325−337.
(21) Liu, Y.; Yang, Z.; Gong, C.; Zhang, L.; Yu, G.; Gong, W. *Cancer Sci.* **2014**, in press.
(22) Nagao, A.; Seki, M.; Kobayashi, H. *Biosci. Biotechnol. Biochem.* **1999**, *63*, 1787−1790.
(23) Pauff, J. M.; Hille, R. *J. Nat. Prod.* **2009**, *72*, 725−731.
(24) Parker, L. J.; Taruya, S.; Tsuganezawa, K.; Ogawa, N.; Mikuni, J.; Honda, K.; Tomabechi, Y.; Handa, N.; Shirouzu, M.; Yokoyama, S.; Tanaka, A. *Acta Crystallogr.* **2014**, *D70*, 392−404.
(25) Shakya, T.; Stogios, P. J.; Waglechner, N.; Evdokimova, E.; Ejim, L.; Blanchard, J. E.; McArthur, A. G.; Savchenko, A.; Wright, G. D. *Chem. Biol.* **2011**, *18*, 1591−1601.
(26) Wiseman, R. L.; Zhang, Y.; Lee, K. P.; Harding, H. P.; Haynes, C. M.; Price, J.; Sicheri, F.; Ron, D. *Mol. Cell* **2010**, *38*, 291−304.
(27) Ugochukwu, E.; Soundararajan, M.; Rellos, P.; Fedorov, O.; Phillips, C.; Wang, J.; Hapka, E.; Filippakopoulos, P.; Chaikuad, A.; Pike, A. C. W.; Carpenter, L.; Vollmar, M.; von Delft, F.; Bountra, C.; Arrowsmith, C. H.; Weigelt, J.; Edwards, A.; Knapp, S. *Structural Genomics Consortium* (unpublished structure in Protein Data Bank).
(28) Zhang, L.; Kong, Y.; Wu, D.; Zhang, H.; Wu, J.; Chen, J.; Ding, J.; Hu, L.; Jiang, H.; Shen, X. *Protein Sci.* **2008**, *17*, 1971−1978.
(29) Trabelsi, N.; Petit, P.; Manigand, C.; Langlois d'Estaintot, B.; Granier, T.; Chaudière, J.; Gallois, B. *Acta Crystallogr.* **2008**, *D64*, 883−391.
(30) Pilka, E. S.; Phillips, C.; King, O. N. F.; Guo, K.; von Delft, F.; Pike, A. C. W.; Arrowsmith, C. H.; Weigelt, J.; Edwards, A. M.; Oppermann, U. *Structural Genomics Consortium* (unpublished structure in Protein Data Bank).
(31) Gledhill, J. R.; Montgomery, M. G.; Leslie, A. G.; Walker, J. E. *Proc. Natl. Acad. Sci. U.S.A.* **2007**, *104*, 13632−13637.
(32) Alguel, Y.; Meng, C.; Teran, W.; Krell, T.; Ramos, J. L.; Gallegos, M. T.; Zhang, X. *J. Mol. Biol.* **2007**, *369*, 829−840.
(33) Holder, S.; Zemskova, M.; Zhang, C.; Tabrizizad, M.; Bremer, R.; Neidigh, J. W.; Lilly, M. B. *Mol. Cancer Ther.* **2007**, *6*, 163−172.
(34) Offen, W.; Martinez-Fleites, C.; Yang, M.; Kiat-Lim, E.; Davis, B. G.; Tarling, C. A.; Ford, C. M.; Bowles, D. J.; Davies, G. J. *EMBO J.* **2006**, *25*, 1396−1405.
(35) Steiner, R. A.; Kalk, K. H.; Dijkstra, B. W. *Proc. Natl. Acad. Sci. U.S.A.* **2002**, *99*, 16625−16630.
(36) Wilmouth, R. C.; Turnbull, J. J.; Welford, R. W. D.; Clifton, I. J.; Prescott, A. G.; Schofield, C. J. *Structure* **2002**, *10*, 93−103.
(37) Walker, E. H.; Pacold, M. E.; Perisic, O.; Stephens, L.; Hawkins, P. T.; Whymann, M. P.; Williams, R. L. *Mol. Cell* **2000**, *6*, 909−919.
(38) Sicheri, F.; Moarefi, I.; Kuriyan, J. *Nature* **1997**, *385*, 602−609.
(39) Pauff, J. M.; Cao, H.; Hille, R. *J. Biol. Chem.* **2009**, *284*, 8760−8767.
(40) Pauff, J. M.; Zhang, J.; Bell, C. E.; Hille, R. *J. Biol. Chem.* **2008**, *283*, 4818−4824.
(41) Cao, H.; Pauff, J. M.; Hille, R. *J. Biol. Chem.* **2010**, *285*, 28044−28053.
(42) Dietzel, U.; Kuper, J.; Doebbler, J.; Schulte, A.; Truglio, J.; Leimkühler, S.; Kisker, C. *J. Biol. Chem.* **2009**, *284*, 8768−8776.
(43) Okamoto, K.; Eger, B. T.; Nishino, T.; Pai, E. F.; Nishino, T. *Nucleosides, Nucleotides Nucleic Acids* **2008**, *27*, 1532−2335.
(44) Cornard, J. P.; Merlin, J. C.; Boudet, A. C.; Vrielynck, L. *Biospectroscopy* **1997**, *3*, 183−193.
(45) Cos, P.; Ying, L.; Calomme, M.; Hu, J. P.; Cimanga, K.; Van Poel, B.; Pieters, L.; Vlietinck, A. J.; Vanden Berghe, D. *J. Nat. Prod.* **1998**, *61*, 71−76.
(46) Pauff, J. M.; Hemann, C. F.; Jünemann, N.; Leimkühler, S.; Hille, R. *J. Biol. Chem.* **2007**, *282*, 12785−12790.
(47) Cao, H.; James, H.; Hille, R. *Biochemistry* **2014**, *53*, 533−541.
(48) Yamaguchi, Y.; Matsumura, T.; Ichida, K.; Okamoto, K.; Nishino, T. *J. Biochem.* **2007**, *141*, 513−524.
(49) Massey, V.; Brumby, P. E.; Komai, H.; Palmer, G. *J. Biol. Chem.* **1969**, *244*, 1682−1691.
(50) Edmondson, D.; Massey, V.; Palmer, G.; Beacham, L. M., III; Elion, G. B. *J. Biol. Chem.* **1972**, *247*, 1597−1604.
(51) Nishino, T.; Nishino, T.; Tsushima, K. *FEBS Lett.* **1981**, *131*, 369−372.
(52) Collaborative Computational Project, Number 4. *Acta Crystallogr.* **1994**, *50D*, 760−763.
(53) Murshudov, G.; Vagin, A.; Dodson, E. J. *Acta Crystallogr.* **1997**, *53D*, 240−255.
(54) Schuettelkopf, A. W.; van Aalten, D. M. F. *Acta Crystallogr.* **2004**, *60D*, 1355−1363.
(55) Emsley, P.; Cowtan, K. *Acta Crystallogr.* **2004**, *60D*, 2126−2132.
(56) DeLano, W. L. *The PyMOL Molecular Graphics System*; Schrödinger, LLC, 2010.
(57) Laskowski, R. A.; MacArthur, M. W.; Moss, D. S.; Thornton, J. M. *J. Appl. Crystallogr.* **1993**, *26*, 283−291.